Abrupt transitions in species number densities and plasma parameters in a CH_3F/O_2 inductively coupled plasma

Erdinc Karakas, Vincent M. Donnelly, and Demetre J. Economou
Plasma Processing Laboratory, Department of Chemical and Biomolecular Engineering, University of Houston, Houston, Texas 77204-4004, USA

(Received 12 December 2012; accepted 10 January 2013; published online 24 January 2013)

Measured relative densities as a function of O_2 addition in a CH_3F/O_2 inductively coupled plasma changed abruptly for H, O, and particularly F atoms (factor of 4) at 48% O_2. A corresponding transition was observed in electron density, effective electron temperature, and gas temperature, as well as in C, CF, and CH optical emission. These abrupt transitions were attributed to the reactor wall reactivity, changing from a polymer-coated surface to a polymer-free surface and vice-versa, as the O_2 content in the feed gas crossed 48%. © *2013 American Institute of Physics*.
[http://dx.doi.org/10.1063/1.4789435]

The complex structure of advanced gate electrode designs for field effect transistors (e.g., FinFET) requires highly anisotropic and selective Si_3N_4 etching over Si. CH_3F/O_2 plasmas have been employed in an effort to satisfy these requirements.[1–4] Despite their importance, studies of these plasmas are scarce. In this letter, CH_3F/O_2 inductively coupled plasmas (ICP) were investigated as a function of gas composition. Surprisingly abrupt transitions of species densities (particularly F atoms) and plasma parameters were observed at 48 vol. % of O_2 addition.

An ICP was sustained in a water cooled (20 °C) 1.4″ ID alumina tube. An ENI radio frequency (rf) amplifier, driven by a Hewlett-Packard function generator, supplied power to a 3-turn, 2.5″ ID coil at 13.56 MHz through a matching network. Forward and reflected powers were measured by inline Bird meters. Pressure was measured at the top flange with a capacitance manometer. The total flow rate was 10 sccm (standard cm^3 per minute), and the percentage of O_2 was varied between 0 and 100%. A small amount (2.5%) of a rare gas mixture containing 40% Ne, 20% Ar, 20% Kr, and 20% Xe was added to the feed gas. Three spectrometers (Ocean Optics HR4000, high resolution) were employed to cover wavelength ranges of 200–427, 578–775, and 764–916 nm. Light was collected along the axis down the center of the cylindrical discharge without a lens or mirror. Unless stated otherwise, the experimental inputs were 300 W (~2 W/cm^3) net power and 10 mTorr pressure.

Optical emission spectra were recorded as a function of O_2 addition. Atomic and molecular emission lines were identified, and the intensities were recorded for H (656.28 nm, $E = 12.03$ eV), F (703.74 nm, $E = 14.6$ eV), O (844.63 nm, $E = 10.94$ eV), C (247.7 nm, $E = 7.65$ eV), CO ($b^3\Sigma^+ \rightarrow a^3\Pi$) (0,1) at 297.74 nm ($E = 10.34$ eV), $CO_2^+(^2\Sigma_u^+ \rightarrow {}^2\Pi_g)$ at 289 nm ($E_{ip} + E = 13.77 + 4.27$ eV), $HF^+(A^2\Sigma^+ \rightarrow X^2\Pi)$ at 390 nm ($E_{ip} + E = 16.04 + 3.14$ eV), $CF(B^2\Delta_r \rightarrow X^2\Pi_r)$ at 202.59 nm ($E = 6.09$ eV), $CH(A^2\Delta \rightarrow X^2\Pi)$ (0,0) at 431.25 nm ($E = 2.86$ eV), and $OH(A^2\Sigma \rightarrow X^2\Pi)$ at 306.4 nm ($E = 4.03$ eV). E_{ip} is the first ionization potential of CO_2 or HF, and E is the energy of the emitting species above its like-charged ground state. These intensities were divided by the intensity of either the Ar 750.3 nm ($E = 13.42$ eV) line (a better match on average for atomic species) or the Xe 834.68 nm ($E = 11.06$ eV) line (better for the average energy of molecular species, especially if ion emission is excited through the ground state of the ion) to at least partially remove the dependence of the emission intensity on the electron number density and energy distribution. As it turns out, it makes little difference whether the Ar or Xe line was used. For some species (i.e., H, F, O, and CO), this actinometry method[5,6] can provide a semi-quantitative measure of relative species-to-rare gas number density ratios. If the electron impact excitation rate constants are known or calibrations can be performed, absolute number densities can be estimated, but this was not done here.

In CH_3F rich-plasmas, a polymer film deposited on the reactor walls. Under these conditions, the plasma reached a steady-state where the optical emission spectrum was constant over time, while the polymer film continued to deposit. To always establish steady-state conditions, when an experiment was done with a CH_3F-rich mixture (e.g., 90/10 CH_3F/O_2), it was followed by the reverse, O_2-rich ratio (i.e., 10/90 CH_3F/O_2). The pressure for this O_2-rich experiment started at ~15 mTorr, as the film from the previous run was being etched from the reactor walls, increasing the number of moles injected into the system, and dropped to a constant 10 mTorr in seconds to minutes (depending on present and prior conditions) as the last patches of the film cleared.

Relative emission intensity ratios for H/Ar, F/Ar, O/Ar, and C/Ar are given in Figure 1 as a function of added O_2. Each data point was the average of three measurements. Emission ratios exhibit an abrupt transition at 48% ± 1%, with F/Ar, O/Ar, and H/Ar exhibiting a sudden increase of 4-fold, 1.8-fold, and 1.4-fold, respectively. Such an unusual abrupt change in atomic number densities has apparently never been reported as the feed gas composition of a plasma is smoothly changed. The C/Ar ratio also has a very unusual, "inverted V" dependence on $\%O_2$. It should be noted that the Ar and Xe emissions in mostly CH_3F plasmas were about the same as those in mostly O_2 plasmas and exhibited broad, shallow dips (~20% in magnitude) near 55% O_2. This indicates that the behavior in emission ratios and therefore atom number densities is due to causes other than changes in the electron density and/or temperature. Molecular emissions intensities, divided by Xe emission intensities, are plotted in

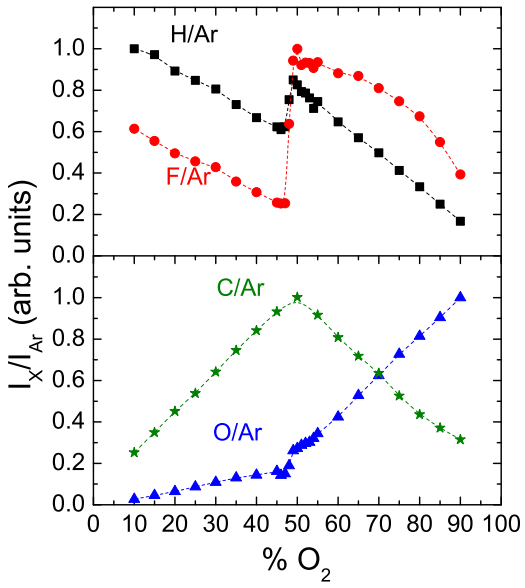

FIG. 1. Relative emission intensity ratios for H/Ar, F/Ar, C/Ar, and O/Ar as a function of O_2 addition to CH_3F feed gas at a constant total flow rate (10 sccm), pressure (10 mTorr), and net power (300 W).

Figure 2 as a function of added O_2. An abrupt transition is also observed for CF/Xe (1.7-fold), as well as CH/Xe, although the change in CH is much milder (1.05-fold). HF^+/Xe and CO/Xe display broad maxima near 50% O_2. The remaining emission ratios CO_2^+/Xe and OH/Xe have similar broad maxima but peak at a higher O_2 percentage (~65% and ~60%, respectively).

Electron energy probability functions (EEPF) between ~2 and 35 eV were obtained with a Langmuir probe. EEPFs of both CH_3F-rich and O_2-rich plasmas exhibited similar bi-Maxwellian shapes with the 2–15 eV region characterized by a relatively high electron temperature (T_e) and the 15–35 eV region exhibiting a colder T_e, likely due to energy losses in high-threshold inelastic electron-neutral collisions. Figure 3(a)

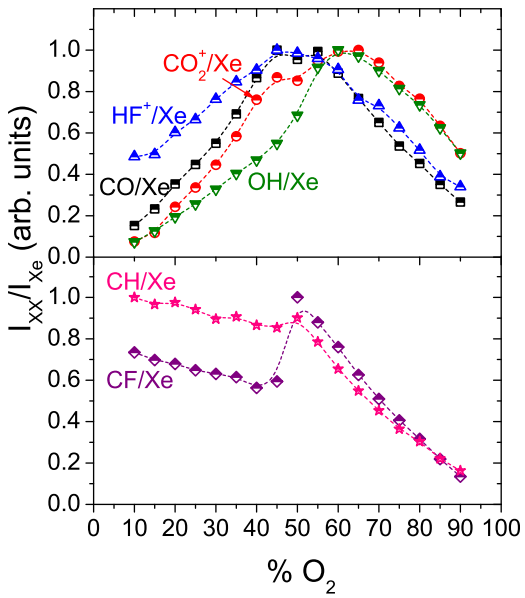

FIG. 2. Relative emission intensity ratios for CO/Xe, CO_2^+/Xe, HF^+/Xe, CF/Xe, CH/Xe, and OH/Xe as a function of O_2 addition to CH_3F feed gas at a constant total flow rate (10 sccm), pressure (10 mTorr), and net power (300 W).

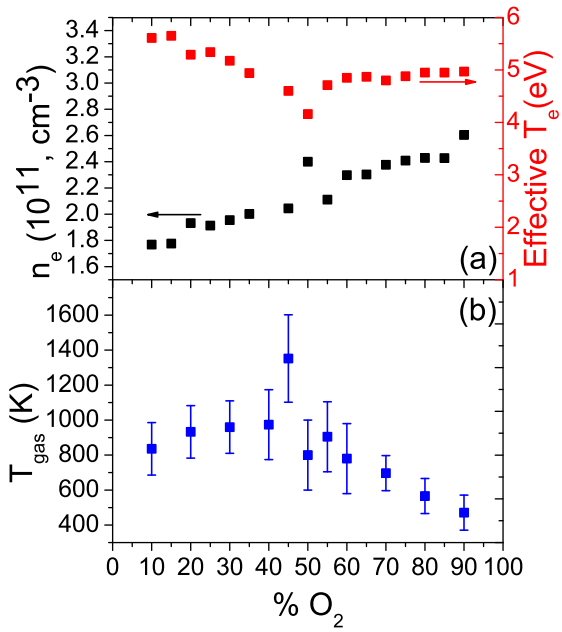

FIG. 3. (a) Electron number density (n_e) and effective electron temperature (T_e), (b) gas temperature (T_{gas}), as a function of O_2 addition to CH_3F feed gas at a constant total flow rate (10 sccm), pressure (10 mTorr), and net power (300 W).

presents electron density (n_e) and effective electron temperature (T_e^{eff}) derived from the EEPF,[7] where $n_e = \int_0^\infty \varepsilon^{\frac{1}{2}} f(\varepsilon) d\varepsilon$ and $T_e^{eff} = 2/3n \int_0^\infty \varepsilon^{\frac{3}{2}} f(\varepsilon) d\varepsilon$.[7] n_e increases from 1.76×10^{11} to 2.6×10^{11} cm^{-3} with a peak near 50% added O_2. T_e^{eff}, reflecting mainly the high energy tail of the EEPF,[7] varies between 4.16 and 5.65 eV, with a minimum at 50% added oxygen.

Gas temperatures (T_{gas}) were measured by adding a small amount (2.5%) of N_2 to the feed gas and recording emission from the second positive system of N_2 ($C^3\Pi_u \rightarrow B^3\Pi_g$). The rotational structure of the (1,0) and (1,3) vibronic bands at 315.9 and 375.5 nm was simulated and matched to observations with T_{gas} as an adjustable parameter.[8,9] T_{gas} was found to be a strong function of the feed gas composition (Figure 3(b)). On the CH_3F-rich side, adding O_2 increases T_{gas} from 800 to 1000 K, most likely resulting from the heat released in exothermic reactions that form CO and CO_2. At 45% O_2, an abrupt rise to 1400 K is observed, then T_{gas} suddenly drops off to ~800 K with slightly more O_2. T_g continues decreasing with further added O_2 until reaching 500 K in a 90% O_2 feed gas plasma, consistent with the diminished production of heat from formation of CO and CO_2.

The falloff in all but O/Ar above 50% to 65% added O_2 is mostly due simply to dilution. The behavior of several emission intensity ratios in CH_3F-rich plasmas and the abrupt transition at 48% O_2 have more involved explanations. In pure CH_3F plasmas, electron impact forms F, H, CH_3, and CH_2F in a nearly statistical ratio.[10] Electron impact of CH_3 and CH_2F also occurs. F abstracts H from CH_3F and the other hydrocarbons in the gas phase and likely from polymer on the surface of the discharge tube. A polymer film can grow on the walls of the reactor when radicals such as CH_3, CH_2F, CH, and CF stick on the surface. As O_2 is added to a CH_3F-rich plasma, F/Ar and H/Ar initially fall nearly as expected from dilution (Figure 1). At the same time, the density of O-atoms (formed by electron impact of O_2) grows

linearly with O_2 feed gas percentage. The CO and OH densities also increase (Fig. 2). CO production can occur through many reactions, including $O + CH_3 \rightarrow CO + H_2 + H$.[11] Furthermore, CO is expected to be a primary product of polymer etching by O atoms. OH-containing species could also be produced in this etching process, as well as through gas phase reactions.

As more O_2 is added to the feed gas, the polymer deposition rate slows by dilution and by reactions that deplete the plasma of deposition precursors such CH and CF (Figure 2). At the same time, the film etching rate increases due to the increase in O-atom number density. Apparently, the film growth rate exceeds the etching rate at less than 48% O_2, while the etching rate exceeds the deposition rate above this O_2 feed gas percentage. Thus, a polymer film covers the discharge tube walls for <48% O_2, while the walls are free of polymer for >48% O_2. Figure 1 also shows that with small additional increases in $\%O_2$ above the 48% transition point, O/Ar increases by a factor of 1.8 (O is no longer consumed in etching), and F/Ar jumps by a factor of 4. T_g also drops sharply between 45 and 50% O_2, as there is no longer a hydrocarbon film on the walls and the heterogeneous production of CO and CO_2 falls off, reducing wall (and gas) heating, and possibly translational or internal energy of desorbing CO and CO_2.

The F/Ar behavior (Figure 1) suggests that the loss rate of F at the walls exceeds that from gas-phase reactions by a factor of 3 on the low-F/Ar side at 48% O_2. Presumably HF is a product of this heterogeneous reaction, yet HF^+/Ar (a surrogate for HF/Ar) undergoes no such step change near 48% (Figure 2). This is because the HF density does not depend on the F-atom density as shown next. For simplicity let us assume that F-atoms are formed by electron impact dissociation of a single CH_xF species with an effective rate coefficient k_1 and are lost by a gas-phase reaction with CH_xF with an effective rate coefficient k_2, as well as by a surface reaction with CH_x on the wall, described by a rate coefficient k_3. Then the steady-state F number density is given by

$$n_F = \frac{k_1 n_{CHxF} n_e}{k_2 n_{CHxF} + k_3 n_{CHw} + k_{pump}}, \quad (1)$$

where n_{CHxF} and n_e are the gas-phase CH_xF and electron number densities, respectively, n_{CHw} is the coverage of CH_x on the walls, and k_{pump} is the rate constant for loss of F (and HF) by pumping. The steady-state HF number density is given by

$$n_{HF} = \frac{k_2 n_{CHxF} + k_3 n_{CHw}}{k_4 n_e + k_{pump}} n_F, \quad (2)$$

where k_4 is the rate coefficient for electron impact dissociation of HF. It is reasonable to assume that $k_2 n_{CHxF} + k_3 n_{CHw} \gg k_{pump}$. Therefore, substituting n_F from Eq. (1) into Eq. (2),

$$n_{HF} = \frac{k_1 n_{CHxF} n_e}{k_4 n_e + k_{pump}}. \quad (3)$$

That is, n_{HF} is independent of F atom number density, and it is not expected to exhibit an abrupt change commensurate with that of F atoms. This is consistent with the behavior of HF^+/Ar in Figure 1. Equation (3) predicts a smooth diluting of n_{HF} with O_2 addition (assuming that n_{CHxF} is proportional to the CH_3F feed gas percentage), yet Figure 2 shows that HF^+/Ar *increases* 2-fold between 5% and 50% O_2 before starting to smoothly decrease. The reason may be that the concentration of HF^+ does not track the concentration of HF. It is also plausible that other channels for the formation of HF open up in the presence of O atoms. For example, reactions $O + CH_2F \rightarrow CO + HF + H$, $O + CHF \rightarrow CO + HF$, and $O + CH_2F \rightarrow COHF + H$ followed by $COHF \rightarrow CO + HF$ would generate HF without producing F (dissociation of COHF could be unimolecular, and/or induced by electron impact). It is noted that some of these reactions will also produce H, but the formation of OH and H_2O removes H, so the net n_H is simply nearly in proportion to the CH_3F feed gas percentage, as observed (Figure 1).

The transition from polymer coated to polymer-free reactor walls, around 48% O_2 addition is corroborated by the data shown in Figure 4. The F/Ar emission intensity ratio (proportional to the F atom density) was followed as a function of time for different % O_2 in the feed. For O_2 additions of 48% and lower, the long time (steady-state) F atom density was suppressed due to reaction with a polymer-coated wall. For O_2 additions of 50% and above, the steady-state F atom density is several times higher, as the reactor walls are polymer-free. The curve for 49% added oxygen in Fig. 4 is right at the transition. At early times, a polymer film grows and the F atom density drops. However, the film is etched at later times, and the F atom density increases. This is one of many possible scenario that can occur at the transition. What actually occurs depends on the starting condition of the wall and may be influenced by seemingly small fluctuations of reactor operating parameters. The transient behavior of each curve in Fig. 4 again depends on the starting condition. For example, the 54% curve was obtained after a run with 46% oxygen. Under these conditions the reactor walls started out with a polymer coating. This is the reason the F atom density is suppressed at early times. However, the polymer film is etched away in the 54% oxygen plasma, and the F atom density eventually saturates at a high value, corresponding to polymer-free walls.

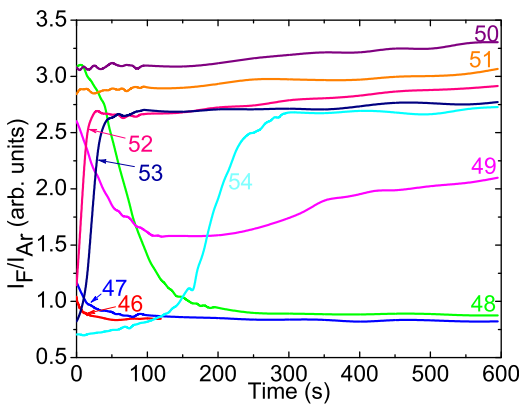

FIG. 4. Time evolution of the F/Ar emission intensity ratio as a function of O_2 addition to CH_3F feed gas at a constant total flow rate (10 sccm), pressure (10 mTorr), and net power (300 W). Experiments were done in the following order: 46%, 54%, 47%, 53%, 48%, 52%, 49%, 51%, and 50% O_2.

Abrupt changes in the plasma composition and parameters of the kind observed in this work have not been reported previously for CH_3F/O_2 or analogous plasmas. Chen *et al.*[1] reported that when O_2 was added to a CH_3F plasma, emission from F and Ar hardly changes for 20, 40, 60, and 80% O_2 addition. It is possible that a smaller step change in F emission occurred at an O_2 percentage between 20 and 80% and was missed because of the coarse grid of O_2 percentages. More likely, a significant step change had occurred in the uninvestigated region of $<20\%$ O_2. When O_2 was added to a CF_4 plasma, the F atom density smoothly increased to a maximum near 20%–50% O_2 addition, due in part to the reaction $O + CF_3 \rightarrow COF_2 + F$ and then decreased due to dilution.[5,12–14] Similarly, smooth changes in F, CF, CF_2, and CF_3 were observed in CHF_3/O_2 plasmas as a function of added O_2.[15] Fujii and Syouji[16] used mass spectrometry to monitor a plethora of ionic and neutral species in a CH_4/O_2 microwave plasma and found only smooth changes in number densities as a function of added O_2. Benndorf *et al.*[17] found no abrupt changes in species concentrations measured by optical emission spectroscopy and mass spectrometry in $CH_4/H_2/O_2$ plasmas when the O_2 partial pressure was varied.

The unique, unusual step-change near 50% O_2 in CH_3F/O_2 plasmas appears to be related to the formation of HF by abstraction of H from a mostly hydrogen-containing coating on the reactor walls. This does not seem to happen to nearly the same extent in fluorine-rich CHF_3/O_2 plasmas and of course cannot happen in CF_4/O_2 plasmas. The large surface-to-volume ratio of the plasma reactor used in the present work may also play a role by making formation of HF by abstraction of surface H from the polymer film a dominant reaction. From the above proposed mechanism, a step change in species number densities, especially n_F, is expected to commonly occur in CH_3F/O_2 plasmas and in plasmas with hydrofluorocarbon feed gases with similar H:F ratios. As long as pure CH_3F plasmas will deposit a polymer film on the walls, there will always be a % O_2 addition where the deposition rate will equal the film etching rate. This % O_2 and the size of the step change in number densities will depend on the reactor geometry, reactor wall temperature, total gas flow rates, pressure, and fraction of the feed gas consumed in the etching of materials such as SiN.

It should be noted that no obvious abrupt changes in the plasma were observed during the transitions. For example, there was no change in the power matching, and no perceptible change by eye in brightness or color. This underscores the importance of monitoring "internal" plasma characteristics (e.g., species densities), as opposed to monitoring only external discharge parameters (power, pressure, etc.).

In summary, inductively coupled CH_3F/O_2 plasmas were investigated as a function of added O_2. It was found that atomic (F, H, and O) number densities undergo an abrupt transition (especially for F) near 48% O_2. This transition was attributed to different wall conditions for CH_3F-rich *vs.* O_2-rich gas mixtures. On the CH_3F-rich side, polymer deposition on the discharge tube surfaces surpasses the rate of etching of the film, leading to one set of heterogeneous chemical reactions. On the O_2-rich side, the film etching rate exceeds the deposition rate, the reactor walls are free of a polymer film, and a different set of heterogeneous reactions occurs. Though not as dramatic, this transition was also seen in some molecular number densities, electron density, effective electron temperature, and gas temperature. The cause of this unique behavior of CH_3F/O_2 plasmas as a function of added O_2, compared to similar plasmas with CF_4, CH_4, or CHF_3 mixtures with O_2, appears related to the abstraction of H by gaseous F from a hydrogen-rich polymer film on the reactor walls.

The authors are grateful to Lam Research and the Department of Energy, Office of Fusion Energy Science (Contract No. DE-SC0001939) for financial support of this work.

[1]L. L. Chen, L. D. Xu, D. X. Li, and B. Lin, Microelectron. Eng. **86**(11), 2354–2357 (2009).
[2]Y. Iijima, Y. Ishikawa, C. Yang, M. Chang, and H. Okano, Jpn. J. Appl. Phys. **36**(Part 1), 5498–5501 (1997).
[3]R. Blanc, O. Joubert, T. David, F. Leverd, and C. Vérove, The Electrochemical Society Abstracts, Abstract No. 2926, Honolulu PRiME 2012, Vol. 39.
[4]O. Joubert, M. Darnon, G. Cunge, E. Pargon, D. Thibault, C. Petit-Etienne, L. Vallier, N. Posseme, P. Bodart, and L. Azarnouche, in *SPIE Advanced Lithography* (International Society for Optics and Photonics, 2012), Vol. 8328, pp. 83280D-1–83280D-10.
[5]J. W. Coburn and M. Chen, J. Appl. Phys. **51**(6), 3134–3136 (1980).
[6]R. A. Gottscho and V. M. Donnelly, J. Appl. Phys. **56**(2), 245–250 (1984).
[7]V. A. Godyak, R. B. Piejak, and B. M. Alexandrovich, Plasma Sources Sci. Technol. **11**(4), 525–543 (2002).
[8]G. P. Davis and R. A. Gottscho, J. Appl. Phys. **54**(6), 3080–3086 (1983).
[9]M. J. Schabel, V. M. Donnelly, A. Kornblit, and W. W. Tai, J. Vac. Sci. Technol. A **20**(2), 555–563 (2002).
[10]S. Motlagh and J. H. Moore, J. Chem. Phys. **109**(2), 432–438 (1998).
[11]P. W. Seakins and S. R. Leone, J. Phys. Chem. **96**(11), 4478–4485 (1992).
[12]C. J. Mogab, A. C. Adams, and D. L. Flamm, J. Appl. Phys. **49**(7), 3796–3803 (1978).
[13]V. M. Donnelly, D. L. Flamm, W. C. Dautremontsmith, and D. J. Werder, J. Appl. Phys. **55**(1), 242–252 (1984).
[14]D. L. Flamm, V. M. Donnelly, and D. E. Ibbotson, in *VLSI Electronics: Microstructure Science*, edited by N. G. Einspruch and D. M. Brown (Academic, 1984), Vol. 8, pp. 189–251.
[15]K. Takahashi, M. Hori, and T. Goto, J. Vac. Sci. Technol. A **14**(4), 2004–2010 (1996).
[16]T. Fujii and K. Syouji, J. Phys. Chem. **97**(44), 11380–11384 (1993).
[17]C. Benndorf, P. Joeris, and R. Kroger, Pure Appl. Chem. **66**(6), 1195–1205 (1994).